Springer

KSME

Journal of Mechanical Science and Technology 24 (10) (2010) 2059~2066
www.springerlink.com/content/1738-494x
DOI 10.1007/s12206-010-0619-6

Performance enhancement of axial fan blade through multi-objective optimization techniques †

Jin-Hyuk Kim[1], Jae-Ho Choi[2], Afzal Husain[1] and Kwang-Yong Kim[1,*]

[1]*Department of Mechanical Engineering, Inha University, 253 Yonghyun-dong, Nam-gu, Incheon 402-751, Rep. of Korea*

[2]*Energy Equipment R&D Team, Samsung Techwin Co., Ltd., 701 Sampyeong-dong, Bundang-gu, Seongnam-si, Gyeonggi-do 463-400, Rep. of Korea*

(Manuscript Received March 1, 2010; Revised June 7, 2010; Accepted June 11, 2010)

Abstract

This paper presents an axial fan blade design optimization method incorporating a hybrid multi-objective evolutionary algorithm (hybrid MOEA). In flow analyses, Reynolds-averaged Navier-Stokes (RANS) equations were solved using the shear stress transport turbulence model. The numerical results for the axial and tangential velocities were validated by comparing them with experimental data. Six design variables relating to the blade lean angle and the blade profile were selected through Latin hypercube sampling of design of experiments (DOE) to generate design points within the selected design space. Two objective functions, namely, total efficiency and torque, were employed, and multi-objective optimization was carried out, to enhance the performance. A surrogate model, Response Surface Approximation (RSA), was constructed for each objective function based on the numerical solutions obtained at the specified design points. The Non-dominated Sorting of Genetic Algorithm (NSGA-II) with local search was used for multi-objective optimization. The Pareto-optimal solutions were obtained, and a trade-off analysis was performed between the two conflicting objectives in view of the design and flow constraints. It was observed that, by the process of multi-objective optimization, the total efficiency was enhanced and the torque reduced. The mechanisms of these performance improvements were elucidated by analysis of the Pareto-optimal solutions.

Keywords: Axial fan blade; Evolutionary algorithm; Surrogate model; Pareto-optimal solutions; Total efficiency; Torque

1. Introduction

Recently computing-power advances have rendered numerical optimization techniques based on three-dimensional Reynolds-averaged Navier-Stokes (RANS) equations practical in the design of turbomachinery blades. Application of such techniques has reduced the number of experimental tests required, and thereby has reduced the time and cost entailed, in turbomachine design.

Efficiency and torque are the important parameters in turbomachine performance measurement. Kim et al. [1] have reported a design optimization method for enhancing the efficiency of a centrifugal compressor impeller, based on four variables defining the design of the impeller hub and shroud contours. Efficiency enhancement through modification of the diffuser geometry in a mixed-flow pump was reported by Kim et al. [2]. Seo et al. [3] introduced design optimization of a low-speed axial fan blade with sweep and lean to enhance efficiency. Samad et al. [4] studied a multi-objective optimization of an axial fan modifying a stacking line of blades, and they attempted to enhance the efficiency and total pressure and to reduce the torque.

An optimization procedure for turbomachinery blade design, as based on the response surface approximation (RSA) model, has been applied by Jang and Kim [5] and Chen and Yuan [6]. Several other studies on shape optimization of turbomachinery blades have been undertaken, with specific emphases on maximum camber [7], camber line [8-9], airfoil thickness [10], thickness location [11], trailing edge (TE) radius [12], and others.

Most turbomachinery designs involve multiple performance objectives, and as such, are typically referred to as multi-objective problems. These problems require, for system optimization, simultaneous consideration of all pertinent objective functions. The fast and elitist Non-dominated Sorting Genetic Algorithm (NSGA-II) of Deb et al. [13] generates a Pareto-optimal solution using evolutionary algorithms. For optimization with the Pareto-optimal design, Keskin and Bestle [14] posited Bezier curve parameterization of blade shape. Marjavaara et al. [15] employed multi-objective optimization algorithms for shape optimization of a hydraulic turbine diffuser. Lotfi et al. [8] reported genetic algorithm (GA)-based optimi-

† This paper was recommended for publication in revised form by Associate Editor Jun Sang Park

* Corresponding author. Tel.: +82 32 872 3096, Fax: +82 32 868 1716
E-mail address: kykim@inha.ac.kr

zation of a low-speed fan cascade using Bezier-curve-selected design variables including thickness distribution and camber line. Benini [16] used multi-objective optimization and a Bezier curve to define blade-section profiles in consideration of the total pressure ratio and adiabatic efficiency, and used these as design objectives for an axial compressor blade. He employed the camber line and a thickness profile as the design parameters. Lastly, Pierret et al. [17] reported multi-disciplinary and multiple-operating-point optimizations for fixed rotor speeds.

In the present work, a hybrid multi-objective evolutionary algorithm (hybrid MOEA) [18] coupled with the RSA model was applied to obtain a global Pareto-optimal front for design of an axial fan blade. Three-dimensional RANS analyses were performed to obtain numerical solutions for the selected design points. The blade shape was optimized by six design variables relating to the blade lean angle and blade profile. Two conflicting objectives, that is, the total efficiency and the torque, were selected for optimization.

2. Numerical analysis

Reynolds-averaged Navier-Stokes (RANS) equations were solved using the Shear Stress Transport model as turbulence closure. The commercial software ANSYS CFX 11.0 [19] consisting of Blade-Gen, Turbo-Grid, CFX-Pre and CFX-Solver applications, was employed in flow analyses. The blade profile was generated in Blade-Gen and exported to Turbo-Grid for mesh generation. The meshed geometry was then imported into CFX-Pre for boundary and initial condition definitions, and finally, the model was run in CFX-Solver, which solves three-dimensional steady incompressible RANS equations. The code uses a finite volume solver that utilizes the coupled algebraic multigrid (AMG) method [19].

An important issue in turbulence modeling is the formulation of near-wall turbulence, which determines the accuracy of the wall shear stress formulation. The shear stress turbulence (SST) model is used as a turbulence closure. The SST model, having the advantages of both k-ω and k-ε, employs the k-ω model at the near-wall and the k-ε model in the bulk flow regions, a blending function ensuring a smooth transition between the two models. Recently, the SST model has been regarded among two-equation turbulence closures as the most accurate model for aerodynamic applications.

The computational domain in which the present simulations were performed for a single passage of an axial fan is shown in Fig. 1. The simulations performed were steady-state, and the working substance was 25°C air. The total pressure at the inlet was set to 1.0atm, and at the outlet, a designed mass flow rate for a single passage was established. The solid surfaces were considered to be hydraulically smooth under no-slip and adiabatic conditions, the periodic conditions were set at the blade passage interfaces, and the tip clearance modeled was 2.0 mm. The major design specifications are listed in Table 1.

A hexahedral grid system was employed as the mesh in the computational domain. A grid-independency test had been carried out to determine the optimal grid number, and a grid of 630,000 points was selected. Fig. 1 shows the grid system structure.

Table 1. Design specifications of axial fan.

Flow Coefficient	0.41
Total Pressure Coefficient	0.30
Rotor Rotation Frequency, rpm	1000
Tip Radius, mm	287.5
Number of blades	9
Hub/Tip Ratio	0.52
Inlet Angle at Rotor Tip, degrees	68.8
Outlet Angle at Rotor Tip, degrees	63.8

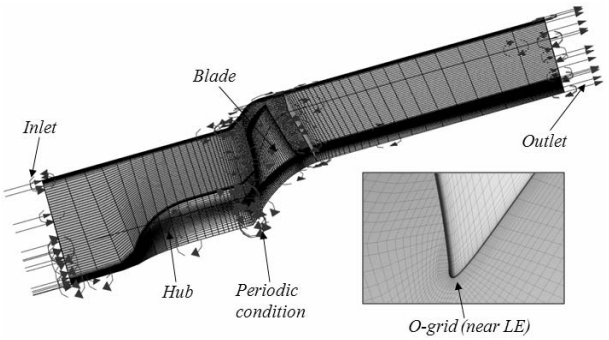

Fig. 1. Computational domain and structure of grid system.

The solutions are made to converge; among the convergence criteria, the root mean square (RMS) residual values of the momentum and mass were set below 1.0E-06, and the imbalances of mass and energy were maintained below 1.0E-03. The converged solutions were obtained after approximately 500 iterations. The computations were carried out using a PC with an Intel Pentium IV CPU with a processing speed of 3.0 GHz. The computation time according to the geometry considered and the rate of convergence was 8-9 hours.

3. Design variables and objective functions

Six design variables were selected from among the various blade profile parameters affecting axial fan performance. These were airfoil maximum camber (α), maximum camber location (β), leading edge (LE) radius (γ), TE radius (δ), lean angle at mid-span (κ) and lean angle at tip span (ξ). The other relevant parameters were kept constant. The blade profile was varied by third-order Bezier curve, as shown in Fig. 2(a). The main advantage of blade curve parameterization by Bezier curves is that a certain limited number of points (the "control points") can be used to control the curves, rendering them smooth and free of discontinuities. By moving these control points, which are considered as design variables, the blade shape can be varied. In the present problem, some of the con-

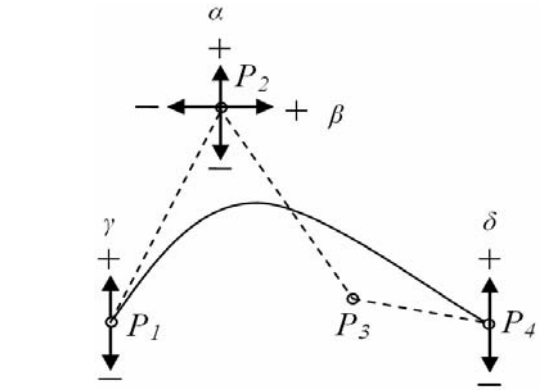

(a) Blade thickness and radius

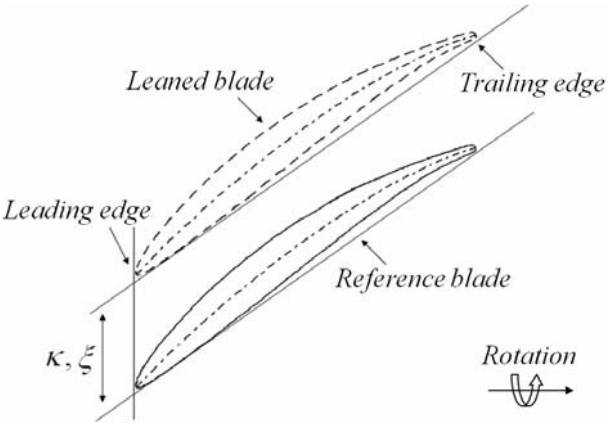

(b) Blade lean

Fig. 2. Definitions of design variables.

trol points were kept fixed so as to reduce the number of design variables.

The curve was defined by a third-order polynomial, and the control points of the Bezier curve were P_1, P_2, P_3 and P_4, P_2, the thickness control point, was moved to change between the design variables α and β. If P_2 was moved vertically, the blade camber (α) was changed, and if P_2 was moved horizontally, the location of maximum camber (β) was changed. In this way, the blade shape was controlled. A positive sign of α indicated an increase of blade thickness, and a similarly positive sign of β indicated movement of the maximum thickness location towards the TE. The LE and TE radii were varied by moving respectively P_1 and P_4 normal to the chord line, the movement being made in such a way that the flow angles did not change. An increase in the positive value of γ and/or δ showed an increase of radius. For the blade lean, the blade tip airfoil was moved normal to the chord line, yielding one design variable; a similar movement of the mid-span airfoil represented another design variable. That is to say, two design variables were used for the blade lean: that for airfoil movements at the blade tip (ξ) and mid-span (κ). Fig. 2(b) illustrates the pertinent definitions of blade lean.

The purpose of this study was to enhance the total efficiency and reduce the required torque of an axial fan blade. Accordingly, total efficiency and torque were selected as the performance parameters in the multi-objective optimization. These objective functions are defined as follows:

- Total efficiency, $\eta=\{(P_{t,\,out}-P_{t,\,in})\cdot Q\}/(\tau\cdot\omega)$.
- Torque, τ.

Here, P_t is the total pressure, and the subscripts *in* and *out* respectively indicate the inlet and exit of the fan. Q is the volume flow rate, and torque is related to input power ($\tau \cdot \omega$) through the constant angular velocity (ω) of the blade. These objective functions were calculated by solving RANS equations at the DOE-specified design points, and a hybrid MOEA was applied to obtain the global Pareto-optimal solutions.

4. Optimization techniques

Any multi-objective optimization based on evolutionary algorithms requires many evaluations of objective functions in searching for Pareto-optimal solutions. Therefore, to evaluate these objective-function values, surrogate-based approximation was utilized, which minimized numerical or experimental expense and saved time. Queipo et al. [20] having suggested the application of various surrogate models, including second-order polynomial approximation, RSA [21] was used in the present study to evaluate the objective function values at the required design sites. RSA is a methodology of fitting a polynomial function for discrete responses obtained from numerical calculations. It reflects the association between response functions and design variables. The constructed second-order polynomial response can be expressed as

$$f(x)=\beta_0+\sum_{j=1}^{N}\beta_j x_j+\sum_{j=1}^{N}\beta_{jj}x_j^2+\sum\sum_{i\neq j}^{N}\beta_{ij}x_i x_j \tag{1}$$

Here, β represents regression analysis coefficients, and $\boldsymbol{x}$ indicates a set of design variables. The multi-objective optimization problem is formulated as

$$\begin{aligned} &\text{Minimize} && \bar{f}(\bar{x}) \quad \text{(M functions to be optimized)}\\ &\text{Subject to} && \bar{g}(\bar{x})\le 0 \quad \text{(s inequality constraints)}\\ &&& \bar{h}(\bar{x})=0 \quad \text{(t equality constraints)} \end{aligned}$$

where $\bar{f}(\bar{x})=\{f_1(\bar{x}),f_2(\bar{x}),f_3(\bar{x}),.....f_M(\bar{x})\}$ is a vector of M real-valued objective functions and x is a vector of N design variables. Thus, $\bar{x}\in R^N$, $\bar{g}(\bar{x})\in R^5$, and $\bar{h}(\bar{x})\in R^t$. In the present problem, there are two conflicting objectives, by which improvement of one objective leads to impairment of the other. Each feasible solution set $\bar{x}$ of the multi-objective problem is either dominated or non-dominated; all non-dominated solutions are called Pareto-optimal solutions. The vector $\bar{x}_i$ dominates a vector $\bar{x}_j$ if $\bar{x}_i$ is at least as good as $\bar{x}_j$ for all objectives and if $\bar{x}_i$ is strictly better than $\bar{x}_j$ for at least one objective.

Objective functions are defined mathematically and evaluated on the experimental data by numerical simulation. A hybrid, multi-objective and evolutionary approach is used to obtain global Pareto-optimal solutions. In this method, first,

approximate Pareto-optimal solutions are obtained using the real-coded NSGA-II developed by Deb [18] for the two objective functions, total efficiency and torque. Here, real-coded indicates that the crossover and mutations are conducted in real space to obtain a response from NSGA-II. The Pareto-optimal solutions are then refined by searching for a local optimal solution for each objective function over all NSGA-II-derived optimal solutions; the search uses Sequential Quadratic Programming (SQP) [22] with NSGA-II solutions as initial guesses. SQP is a generalization of Newton's method, which is a gradient-based optimization technique. To perform a local search, usually two approaches are applied [18]. In one approach, all objectives are combined into a single composite objective, and the optimum is searched. In the other approach, one objective is optimized by treating the others as equality constraints, and the process is repeated for all objectives.

In the present study, the first objective was optimized, and the second objective was treated as an equality constraint. The local search was repeated for the second objective function by treating the first as an equality constraint. This process yielded two new sets of optimal solutions, which were then merged with the NSGA-II solutions. From these solutions, the dominated solutions were discarded and then the duplicate solutions were removed so as to obtain the global Pareto-optimal solutions. Subsequently, the process of local search improved the quality of the Pareto-optimal solutions. In order to find representative solutions from the Pareto-optimal front, K-means clustering [23] was performed. This is an iterative alternating fitting process to form a number of specified clusters. These representative solutions were then distributed along the Pareto-optimal front.

5. Results and discussion

The numerical results of the flow analysis had been validated prior to the flow analysis and design optimization. The numerical results were validated with the test data from the axial fan performance testing [24], and were considered as a reference model. Fig. 3 shows the results of the validation for distributions of the axial and tangential velocity components. The normalized axial and tangential velocity distributions are plotted along the normalized spanwise direction. The two velocity distributions show good agreement with the test data.

In design optimization, it is important to find the feasible design space, which is formed by ranges of design variables. The ranges of design variables, set subject to the experimental and design constraints, are listed in Table 2.

The RSA was trained for both objective functions using the RANS-derived solutions at the discrete design points. In the RSA method, an analysis of variance (ANOVA) and a regression analysis, replete with t-statistics [21], are implemented to measure the uncertainty in a set of coefficients in a polynomial. The values of R^2 and R^2_{adj} for second-order curve-fitting and the RMS error for the surrogate model RSA are listed in Table 3. These values are reliable, according to the $0.9<R^2_{adj}<1.0$ range suggested by Giunta [25] for accurate prediction of the response surface model. Leave-one-out cross-validation [20] was performed to assess the accuracy of the models. Although it is uncertain how well the cross-validation correlated with the model accuracy, the estimation of the generalization errors was nearly unbiased, as it took into account the cross-validation of the surrogate at every design point. The estimations of the cross-validation errors are shown in Table 3.

Table 2. Ranges of design variables.

Variables	Lower	Upper
α (mm)	-4.0	4.0
β (mm)	-12.0	12.0
γ (mm)	-0.5	1.0
δ (mm)	-0.75	0.5
κ (deg)	-15.06	16.94
ξ (deg)	-6.85	10.15

Table 3. Results of ANOVA and regression analysis.

Objective functions	R^2	R^2_{adj}	RMSE	Cross-validation errors
η	0.969	0.920	1.03E-3	1.97E-3
τ	0.999	0.998	3.92E-4	7.15E-4

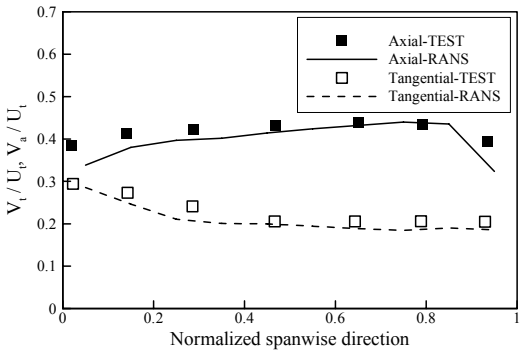

Fig. 3. Validation of flow analysis.

A real-coded NSGA-II was invoked to obtain well-spread, approximate Pareto-optimal solutions with 100 generations and 250 populations. The crossover and mutation probabilities were set to 0.95 and 0.25, respectively. The crossover and mutation parameters were established as 10 and 50, respectively. These parameters were individually adjusted to suit the nature of the problem. Fig. 4 shows the global Pareto-optimal solutions that were generated by the hybrid MOEA through the RSA model, along with the cluster points. Since the efficiency was maximized and the torque minimized, the obtained Pareto-optimal solutions resembled a convex front, and for every fixed value of one objective function, there was one optimal value of the other objective function. Each extreme end of the Pareto-optimal front represents a pair of either the lowest values or the highest values of the two objective functions. Since the objective functions are conflicting in nature,

Table 4. Results of design optimization.

Design	Design variables						MOEA prediction		CFD calculation		Increment	
	α (mm)	β (mm)	γ (mm)	δ (mm)	κ (deg)	ξ (deg)	τ	η	τ	η	τ (%)	η (%P)
Reference	0	0	0	0	0	0	-	-	0.474	0.8557	-	-
Cluster A	3.51	0.04	0.32	-0.75	16.94	8.46	0.297	0.8193	0.283	0.8051	67.71 ↓	5.06 ↓
Cluster B	1.67	0.04	0.29	-0.75	16.40	10.14	0.342	0.8396	0.332	0.8353	42.93 ↓	2.04 ↓
Cluster C	-0.69	0.04	0.36	-0.75	10.94	10.15	0.398	0.8566	0.397	0.8541	19.48 ↓	0.16 ↓
Cluster D	-2.30	0.04	0.73	-0.53	9.19	10.15	0.436	0.8629	0.437	0.8613	8.47 ↓	0.56 ↑

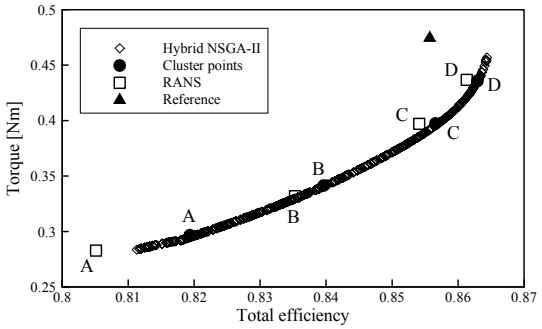

Fig. 4. Pareto-optimal solutions by hybrid MOEA.

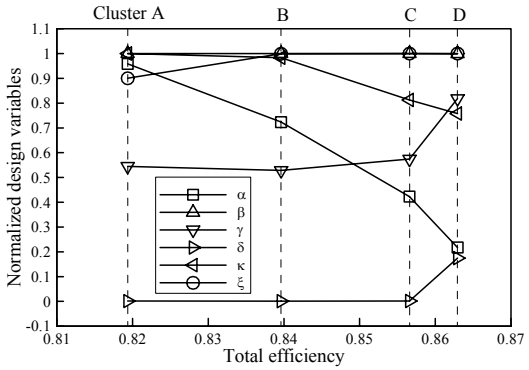

Fig. 5. Distributions of design variables over cluster points with total efficiency.

the improvement of one objective leads to the impairment of the other. Here, it can be seen that no solution out of the Pareto-optimal solutions is superior to any other, in either objective, since each solution is a global Pareto-optimal solution. A trade-off analysis showed that a higher efficiency can be obtained at the cost of a higher torque, whereas the lower torque values are associated with lower values of efficiency. A designer can choose any optimal solution that accords with the available power that delivered the torque required for driving the fluid.

A greater insight into the relationship between the objective function and the design variables was attained by analyzing the Pareto-sensitivity of the design variables, which is to say, the change in the values of the design variables with the change in the objective-function (e.g. total efficiency) values along the Pareto-optimal front. Out of the 620 global Pareto-optimal solutions, 4 clusters, A, B, C and D, were formed to find the representative Pareto-optimal solutions, as shown in Fig. 4. Fig. 5 illustrates the RSA-predicted Pareto-sensitivity of the design variables for those representative Pareto-optimal solutions. The Pareto-sensitivity analysis not only revealed the effectiveness of the design variables but also determined the extremes of the active design space in the Pareto-optimal design paradigm. The two design variables α and κ showed a decreasing trend, whereas the three design variables γ, δ, and ξ revealed an increasing trend. However, β was almost constant with efficiency. Thus, higher efficiency, in the context of the Pareto-optimal designs, was obtained for low values of α and κ and high values of γ, δ and ξ. The design variable β showed the least sensitivity to objective functions along the Pareto-optimal front. This design variable, then, can suitably be utilized to economize the procedure for multi-variable, multi-objective and multi-disciplinary design optimizations requiring simultaneous consideration of many design variables and many performance objectives.

The cluster solutions were reproduced by means of a RANS analysis, as shown in Table 4. All of the representative optimal designs indicated that there was a significant decrease in the torque, though only a relatively small decrease of efficiency was associated with them. In order to determine the main factors responsible for the increase in the objective functions, the internal flow fields were compared with the reference model and the optimal designs A and D.

Fig. 6 shows the distributions of the torque value at the blade. The maximum torque value for solution A was observed near the 70% blade span, whereas for the other designs it was observed near the 80% span. Designs A and D had lower torque values along the blade spans of 20~90% and 20~70%, respectively, than did the reference model. However, for the blade spans beyond 90%, their torque values were higher.

Fig. 7 shows the pressure distributions along the blade spans of 10%, 50% and 90% for the suction and pressure surfaces in the reference model and optimal models A and D. On the whole, the pressure distribution in model A, with the lowest torque, has the lowest values among the three models. However, it also had the highest pressure values for blade LE. The pressure distribution of the pressure surface in model D was

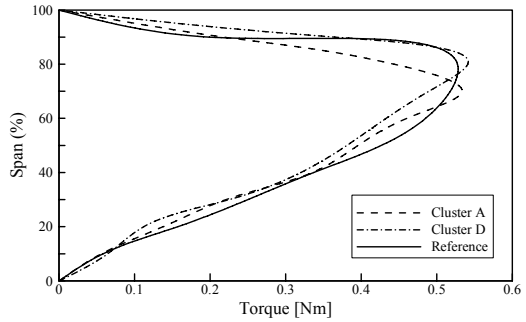

Fig. 6. Comparison of blade torques.

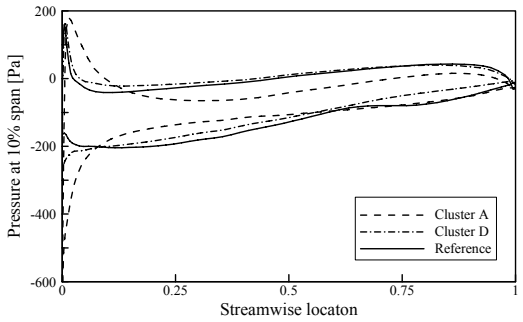

(a) At 10% span

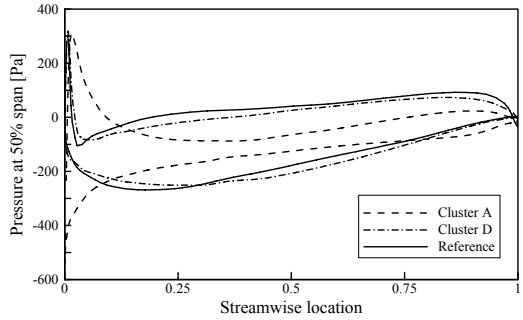

(b) At 50% span

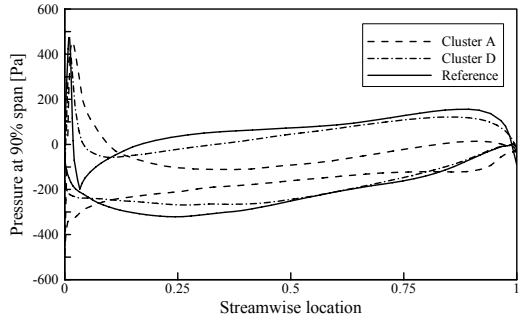

(c) At 90% span

Fig. 7. Pressure distributions on blade surfaces.

entirely more uniform than in the case of the reference model. This trend was caused by the variation of the incidence angle with the changes of the design variables.

Fig. 8 shows the streamline distributions on the near-hub plane and the blade suction surface for the reference model and the optimal models A and D. The reference model had the widest recirculation zone at the near-hub and blade suction surface, and diagonal streamlines. But the optimal model A had almost no separation zone at the suction surface; the optimal model D, moreover, had a smaller separation zone than the reference model. Therefore, it is clear that optimized shapes have more stable flow fields.

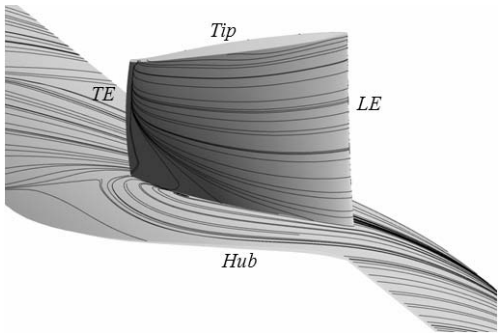

(a) Reference

(b) Cluster A

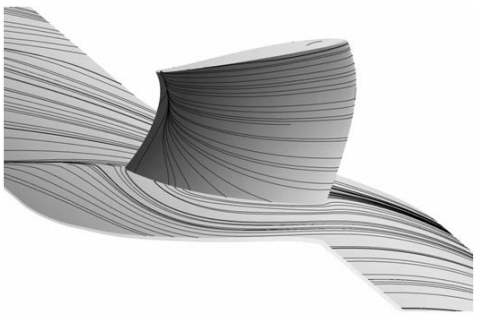

(c) Cluster D

Fig. 8. Streamline distributions on near-hub and blade suction surface.

As discussed above, the optimal designs showed improvement in torque, whereas the total efficiency was increased in the optimal model D and decreased in the optimal model A, compared with the reference model. It is thought that the design variables were changed with the variation in the incidence angle (see Fig. 5), resulting in a significant reduction in the torque and an equally impressive enhancement of the efficiency.

6. Conclusions

Multi-objective optimizations of an axial fan blade were achieved by RSA and a GA with a three-dimensional RANS analysis. Two conflicting objectives, that is, the total efficiency and the torque, were selected for the design optimization. The numerical results were validated with reference to experimental data on the distributions of the axial and tangential velocity components. Six design variables relating to the blade lean angle and the blade profile were modified to enhance the total efficiency and to reduce the torque. According to the Pareto-sensitivity of the design variables, higher efficiency was obtained for high values by LE radius, TE radius and lean angle at the tip span. Two optimal designs, at the extreme ends of total efficiency and torque in the Pareto-optimal front, showed that the efficiencies were increased by 0.56% and decreased by 5.06%, respectively, and that the torques were reduced by 8.47% and 67.71%, respectively, in comparison with the reference model. Therefore, a designer can select, with regard to the reference models and the Pareto-optimal solutions obtained in this work, trade-off designs that are better in both total efficiency and torque. The results show that the present optimization method of hybrid MOEA coupled with RANS analysis can be an efficient tool in design optimization for total efficiency and torque.

Acknowledgment

This research was supported by a Korea Institute of Industrial Technology Evaluation and Planning (ITEP) grant (No. 10031771) funded by the Ministry of Knowledge Economy.

Nomenclature

M : Number of objective functions
$P_{1\text{-}4}$: Control points
$P_{in,\ out}$: Total pressure at inlet and outlet, respectively
Q : Volume flow rate
R^2 : Coefficient of multiple determination
R^2_{adj} : Adjusted value of R^2
RMSE : Root mean square (RMS) error
U_t : Velocity of rotor tip
$V_{a,\ t}$: Axial and tangential velocity, respectively
α : Maximum camber
β : Maximum camber location
γ : Leading edge (LE) radius
δ : Trailing edge (TE) radius
η : Total efficiency
κ : Lean angle at mid-span
ξ : Lean angle at tip span
τ : Torque

References

[1] J. H. Kim, J. H. Choi and K. Y. Kim, Design optimization of a centrifugal compressor impeller using radial basis neural network method, *Proc. of ASME Turbo Expo 2009*, Florida, USA (2009) GT2009-59666.

[2] J. H. Kim, H. J. Ahn and K. Y. Kim, High-efficiency design of a mixed-flow pump, *Science China : Technological Sciences*, 53 (1) (2010) 24-27.

[3] S. J. Seo, S. M. Choi and K. Y. Kim, Design optimization of a low-speed fan blade with sweep and lean, *Proc. of IMechE, Part A: J. Power and Energy*, 222 (1) (2008) 87-92.

[4] A. Samad, K. S. Lee and K. Y. Kim, Multi-objective shape optimization of an axial fan blade, *Int. J. Air-Conditioning and Refrigeration*, 16 (1) (2008) 1-8.

[5] C. M. Jang and K. Y. Kim, Optimization of a stator blade using response surface method in a single-stage transonic axial compressor, *Proc. of IMechE, Part A: J. Power and Energy*, 219 (8) (2005) 595-603.

[6] B. Chen and X. Yuan, Advanced aerodynamic optimization system for turbomachinery, *ASME J. Turbomach*, 130 (2008) 1-12.

[7] K. N. Chung, Y. I. Kim, J. H. Sung, I. H. Chung and S. H. Shin, A study of optimization of blade section shape for a steam turbine, *ASME Fluids Engineering Division Summer Meeting and Exibition*, Texas, USA (2005) FEDSM2005-77385.

[8] O. Lofti, J. A. Teixeira, P. C. Ivey, G. Sheard and I. R. Kinghorn, Aerodynamic optimization of industrial fan blades, *Proc. of ASME Turbo Expo 2005*, Nevada, USA (2005) GT2005-68385.

[9] S. Buruguburu, C. Toussaint, C. Bonhomme and G. Leory, Numerical optimization of turbomachinery bladings, *ASME J. Turbomach*, 126 (2004) 91-100.

[10] C. Xu and R. S. Amano, A turbomachinery blade design and optimization procedure, *Proc. of ASME Turbo Expo 2002*, Amsterdam, Netherlands (2002) GT 2002-30541.

[11] N. Chen, H. W. Zhang, H. Du, Y. J. Xu and W. G. Huang, Effect of maximum camber location on aerodynamics performance of a transonic compressor blade, *Proc. of ASME Turbo Expo 2005*, Nevada, USA (2005) GT2005-68541.

[12] T. Mengistu, W. Ghaly and T. Mansour, Aerodynamic shape optimization of a turbine blades using design-parameter-based shape representation, *Proc. of ASME Turbo Expo 2007*, Montreal, Canada (2007) GT2007-28041.

[13] K. Deb, S. Agrawal, A. Pratap and T. Meyarivan, A fast and elitist multi-objective genetic algorithm for multi-objective optimization: NSGA-II, *Proceeding of the Parallel Problem Solving from Nature VI Conference*, Paris, France (2000) 849-858.

[14] A. Keskin and D. Bestle, Application of multi-objective optimization to axial compressor preliminary design, *Aerospace Science and Technology 10*, (2006) 581-589.

[15] B. D. Marjavaara, T. S. Lundstrom, T. Goel, Y. Mack and W. Shyy, Hydraulic turbine diffuser shape optimization by multiple surrogate model approximations of Pareto Fronts, *Trans. ASME*, 129 (9) (2007) 1228-1240.

[16] E. Benini, Three-dimensional multi-objective design opti-

mization of a transonic compressor rotor, *AIAA Journal of Propulsion and Power*, (20) (3) (2004) 559-565.
[17] S. Pierret, R. F. Coelho and H. Kato, Multidisciplinary and multiple operating points shape optimization of three-dimensional compressor blades, *Structural and Multidisciplinary Optimization*, 33 (1) (2007) 61-70.
[18] K. Deb, Multi-objective optimization using evolutionary algorithms, 1st ed. John Wiley & Sons Inc. Chichester, England (2001).
[19] ANSYS CFX-11.0, Solver Theory, Ansys Inc. (2006).
[20] N. V. Queipo, R. T. Haftka, W. Shyy, T. Goel, R. Vaidyanathan and P. K. Tucker, Surrogate-based analysis and optimization, *Progress in Aerospace Science*, 41 (2005) 1-28.
[21] R. H. Myers and D. C. Montgomery, Response surface methodology: process and product optimization using designed experiments, John Wiley & Sons, Inc., New York, USA (2005).
[22] MATLAB®, The language of technical computing, Release 14, The Math Works Inc. (2004).
[23] JMP 6.0.0, The statistical discovery software, version 6.0.0, SAS Institute Inc., Cary, NC, USA (2005).
[24] C. M. Jang, D. Sato and T. Fukano, Experimental analysis on tip leakage and wake flow in an axial flow fan according to flow rates, *ASME J. of Fluids Eng*., 127 (2005) 322-329.
[25] A. A. Giunta, Aircraft multidisciplinary design optimization using design of experimental theory and response surface modeling methods; Ph.D. dissertation, Virginia Polytechnic Institute and State University, Virginia (1997).

Jin-Hyuk Kim received his bachelor's degree to be honored with the early graduation of excellent from Sunmoon University, Korea, in 2007, and his master's degree from Inha University, Korea, in 2009. He also received the excellent master's thesis award in fluid engineering division from Korean Society of Mechanical Engineers (KSME), Korea. Currently he is pursuing his research towards Ph.D. degree in Thermodynamics and Fluid Mechanics at Inha University, Korea. His research interests are designs of turbomachinery, numerical analyses and optimization techniques.

Jae-Ho Choi received his B.S. degree from Inha University, Korea, in 1993, and his M.S. and Ph.D. degrees in Thermodynamics and Fluid Mechanics at the same University in 1995 and 2000, respectively. He is currently a principal research engineer and the leader of aerodynamic design group at Samsung Techwin R&D Center, Seongnam, Korea. He is an editor in the compressor division of the Korean Fluid Machinery Association (KFMA). His research and development interests are aerodynamic designs with conventional approaches and numerical optimizations, flow analyses, and performance tests on axial-, centrifugal-, and mixed-flow compressors used for energy equipment systems and gas turbines.

Afzal Husain received B.E. and M.Tech. degrees in Mechanical Engineering with specialization in Thermal Sciences from Aligarh Muslim University, India in 2003 and 2005, respectively. He successfully completed Ph.D. degree in Thermodynamics and Fluid Mechanics at Inha University, Republic of Korea. His research interests are computational fluid dynamics, numerical analysis and optimization of fluid flow and heat transfer systems using surrogate models, development of heat transfer augmentation and optimization techniques for conventional- and micro-systems, thermal analysis of micro-electromechanical systems (MEMS), and electronic cooling.

Kwang-Yong Kim received his B.S. degree from Seoul National University in 1978, and his M.S. and Ph.D. degrees from the Korea Advanced Institute of Science and Technology (KAIST), Korea, in 1981 and 1987, respectively. He is currently an Inha Fellow Professor and the head of the School of Mechanical Engineering of Inha University, Incheon, Korea. Professor Kim is also the current editor-in-chief of the International Journal of Fluid Machinery and Systems (IJFMS), and the president of the Korean Fluid Machinery Association (KFMA). He is also a fellow of the American Society of Mechanical Engineers (ASME) and an associate fellow of the American Institute of Aeronautics and Astronautics (AIAA).